

# Hydrophobic hydration and molecular association in methanol–water mixtures studied by microwave dielectric analysis

Takaaki Sato and Akio Chiba

*Department of Applied Physics, School of Science and Engineering, Waseda University, Okubo, Shinjuku-ku, Tokyo 169-8555, Japan*

Ryusuke Nozaki

*Division of Physics, Graduate School of Science, Hokkaido University, Sapporo 060-0810, Japan*

(Received 9 July 1999; accepted 5 November 1999)

Dielectric relaxation measurements on the methanol–water mixtures for the entire concentration range were carried out using time domain reflectometry in the frequency range from 500 MHz to 25 GHz at 20, 25, and 30 °C. The excess partial molar activation free energy, enthalpy, and entropy for methanol,  $\Delta G_{MA}^E$ ,  $\Delta H_{MA}^E$ , and  $\Delta S_{MA}^E$ , and those for water,  $\Delta G_W^E$ ,  $\Delta H_W^E$ , and  $\Delta S_W^E$ , were calculated from accurately measured concentration and temperature dependence of the dielectric relaxation time of the mixtures. The behavior of the excess partial molar quantities in the regions below and above  $X$  (molar fraction of methanol)  $\sim 0.3$  are quite different from each other. In a water-rich region,  $\Delta H_{MA}^E$  and  $\Delta S_{MA}^E$  exhibit two maxima at  $X \sim 0.045$  and  $X \sim 0.12$ , which is clearly attributed to structural enhancement of the hydrogen bond network of water, the so-called hydrophobic hydration. Appearance of two maxima in  $\Delta H_{MA}^E$  and  $\Delta S_{MA}^E$  implies that water molecules surround methanol molecules in qualitatively different manners around the two points. In the concentrated region of  $X \geq 0.3$ , the values of  $\Delta H_{MA}^E$  and  $\Delta S_{MA}^E$  become nearly zero, which means that methanol molecules in the mixtures find themselves in not a very different environment from that in pure methanol, associated and forming chainlike clusters. Water molecules seem to exothermically attach to the hydrophilic site of methanol. © 2000 American Institute of Physics. [S0021-9606(00)52105-9]

## I. INTRODUCTION

Alcohol–water mixtures have been extensively investigated using various experimental and theoretical methods.<sup>1–15</sup> As alcohol molecules have both hydrophilic and hydrophobic groups, the way of dissolution in water is highly complicated. Abnormalities in various properties considered to be structural in origin were observed.<sup>1–8,12–15</sup> There has been a lot of evidence that mixing schemes of alcohol and water drastically change depending on small increments of the concentration of alcohol.<sup>1–15</sup> Dielectric analysis<sup>12–21</sup> is one of the powerful methods, providing information on molecular dynamics. In a previous paper,<sup>12</sup> we have reported the results of dielectric study on ethanol–water mixtures in detail, and discussed dynamical aspects of mixing schemes of ethanol and water in terms of the excess partial molar activation free energy, enthalpy, and entropy for each component, ethanol and water. New information on hydrophobic hydration and molecular association of ethanol has been obtained.

The purpose of this study is to clarify the dynamical structures of methanol–water mixtures. We present accurately measured new data for the mixtures for the entire concentration range with very small increments at three different temperatures of 20, 25, and 30 °C. This paper is a sequel to the previous report on the ethanol–water system,<sup>12</sup> in a series of investigations on interactions between various alcohols and water depending on the size and the shape of the hydrophobic group through molecular dynamics. Dynamical as-

pects of mixing schemes of methanol and water will be discussed in detail in terms of the excess partial molar activation free energy, enthalpy, and entropy for methanol  $\Delta G_{MA}^E$ ,  $\Delta H_{MA}^E$ , and  $\Delta S_{MA}^E$ , and those for water,  $\Delta G_W^E$ ,  $\Delta H_W^E$ , and  $\Delta S_W^E$ . These quantities correspond to the substantial contributions of each component to the excess activation free energy  $\Delta G^E$ , enthalpy  $\Delta H^E$ , and entropy  $\Delta S^E$  of the dielectric relaxation process of the mixtures.<sup>12</sup>

## II. EXPERIMENT

Grade reagent of methanol was purchased from Wako Chemical Co. Ltd. Water was carefully purified by deionization and double distillation, and was used for the measurements immediately after the purification.

Detailed explanations for the apparatus and the measurement procedures have been already reported in a previous paper.<sup>16,20</sup> Dielectric relaxation measurements were carried out using TDR for water–methanol mixtures in the frequency range 500 MHz to 25 GHz at 20, 25, and 30 °C. A flat-end capacitor cell with  $gd = 0.138$  mm was employed for all the measurements. The concentration of the mixture,  $X$ , is defined by the molar fraction of methanol.

## III. RESULTS

### A. Data analysis

A least-squares best fitting procedure was performed by using various models represented by the following function:

$$\varepsilon^*(\omega) = \varepsilon_\infty + \sum_{j=1}^n \frac{\Delta\varepsilon_j}{[1 + (j\omega\tau_j)^{\beta_j}]^{\alpha_j}}, \quad (1)$$

$$\varepsilon_{0j} - \varepsilon_{\infty j} = \Delta\varepsilon_j, \quad 0 < \alpha_j, \beta_j \leq 1,$$

where  $n$  is the number of separable dispersion steps,  $\varepsilon^*(\omega)$  is the complex permittivity, and  $\varepsilon_{0j}$  and  $\varepsilon_{\infty j}$  are the low- and high-frequency permittivity limits for the  $j$ th process from the lower frequency side, respectively.  $\varepsilon_{\infty n} = \varepsilon_\infty$ ,  $\omega$  is an angular frequency, and  $\tau_j$  is the dielectric relaxation time for the  $j$ th process.  $\alpha$  and  $\beta$  are the shape parameters representing asymmetric and symmetric distribution of relaxation times, respectively. Equation (1) includes the Debye ( $\alpha_j = 1$ ,  $\beta_j = 1$ ,  $n = 1$ ; D1), the Cole–Cole ( $\alpha_j = 1$ ,  $0 < \beta_j \leq 1$ ,  $n = 1$ ; CC1), the Davidson–Cole ( $0 < \alpha_j \leq 1$ ,  $\beta_j = 1$ ,  $n = 1$ ; DC1), the Havriliak–Negami ( $0 < \alpha_j \leq 1$ ,  $0 < \beta_j \leq 1$ ,  $n = 1$ ; HN1), the double-Debye ( $\alpha_j = 1$ ,  $\beta_j = 1$ ,  $n = 2$ ; D2), the double Cole–Cole ( $\alpha_j = 1$ ,  $0 < \beta_j \leq 1$ ,  $n = 2$ ; CC2), and so on. Equation (1) was fitted to the measured permittivities by the least-squares best fitting procedure to obtain the absolute minimum value of the normalized variance  $V_{\text{norm}}$ , defined as

$$V_{\text{norm}} = \frac{1}{N} \left[ (1/\varepsilon'_{\text{max}}) \sum_{i=1}^N \delta\varepsilon'(\omega_i)^2 + (1/\varepsilon''_{\text{max}}) \sum_{i=1}^N \delta\varepsilon''(\omega_i)^2 \right], \quad (2)$$

where  $\delta\varepsilon'(\omega_i)$  and  $\delta\varepsilon''(\omega_i)$  are the residuals for dispersion and absorption.  $N$  denotes the number of measured points of permittivity.

## B. Pure water and methanol

We have already reported the results of water.<sup>12,16</sup> The static permittivities  $\varepsilon_0$  at 20,<sup>12</sup> 25,<sup>12,16</sup> and at 30 °C obtained from optimum fitting agree closely with  $\varepsilon_0$  data in the literature<sup>21</sup> within 1%. The fast process ( $j=2$ ) for water characterized by  $\tau_2$  around 1–2 ps,<sup>18,19</sup> which is attributed to hydrogen bond formation and decomposition, is far outside of our accessible frequency range. The single Debye model suffices to fit the data.<sup>12,16</sup> The relaxation time for the main process,  $\tau_1$ , at 25 °C<sup>12,16</sup> accords with the literature values<sup>17–19</sup> within 0.5%, and those at 20 °C<sup>12</sup> and at 30 °C within 1%.

Dielectric relaxation data for methanol measured by TDR up to 25 GHz at 25 °C is shown in Fig. 1. The static permittivities  $\varepsilon_0$  for methanol at 20, 25, and 30 °C obtained from the fitting procedure agree closely with  $\varepsilon_0$  data determined with high-precision capacitance measurements<sup>22</sup> within 1%. In the limited frequency range below 4 GHz, the single Debye model well reproduces the data ( $\log \tau_1 = -10.291$ ,  $\Delta\varepsilon = 26.59$ ,  $\varepsilon_\infty = 6.0$ ,  $\alpha = \beta = 1$ , at 25 °C). In this case, a quite large value of  $\varepsilon_\infty \sim 6.0$  is required. If the full data measured up to 25 GHz are fitted, fitting curves systematically deviate from the data points above 4 GHz. The residuals defined by  $\delta\varepsilon = \varepsilon_{\text{observed}} - \varepsilon_{\text{fit}}$  for dispersion and for absorption are negative and positive, respectively, which is the same trend as the case of the single Debye fit for pure ethanol.<sup>12</sup> The dielectric loss curve of methanol is in appearance asymmetric and broader on the high-frequency side.

It has been assigned that three distinct relaxation processes exist in dielectric relaxation of various alcohols such

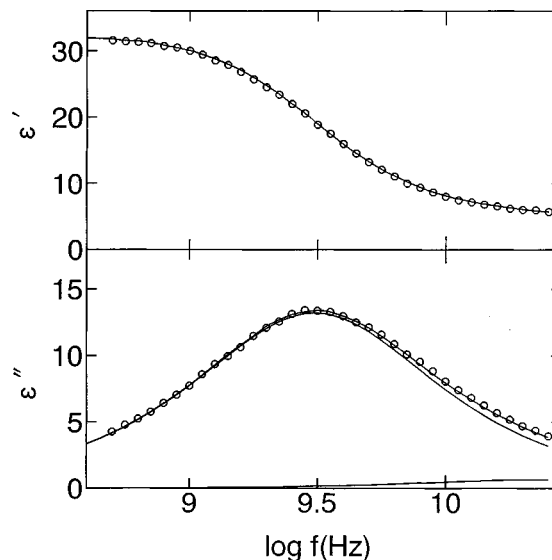


FIG. 1. Frequency dependence of dispersion ( $\varepsilon'$ ) and absorption ( $\varepsilon''$ ) for pure methanol at 25 °C. Symbols  $\circ$  represent the experimental values by using TDR expressed in 0.05 steps in  $\log f$ . The solid curves are calculated from Eq. (1).

as methanol, ethanol, 1-propanol, and 2-propanol.<sup>18,19</sup> We have already reported that dielectric relaxation of ethanol measured up to 25 GHz can be well described only by the double-Debye ( $\alpha_j = 1$ ,  $\beta_j = 1$ ,  $n = 2$ ) model.<sup>12</sup> The fast process ( $j=3$ ) characterized by  $\tau_3$  around 1–2 ps<sup>18,19</sup> is far outside of our accessible frequency range, but our frequency range and the quality of the spectra are sufficient to cover the intermediate process ( $j=2$ ). The double-Debye fit for methanol ( $\log \tau_1 = -10.291$ ,  $\Delta\varepsilon_1 = 26.45$ ,  $\log \tau_2 = -11.14$ ,  $\Delta\varepsilon_2 = 1.27$ ,  $\varepsilon_\infty = 4.8$ , at 25 °C) as well as ethanol agrees quite well with the results by Barthel *et al.*<sup>18,19</sup> Dielectric loss peak frequencies  $f_1 (= 1/2\pi\tau_1)$  and  $f_2 (= 1/2\pi\tau_2)$  for methanol are closer than those for ethanol, which seems to give smaller variance for the Davidson–Cole (DC1) fit for methanol, as indicated by<sup>5</sup> and<sup>6</sup> in Table I.

If the Barthel value of  $\varepsilon_\infty = 2.79$  for methanol<sup>18,19</sup> determined with the data up to 293 GHz is used to fit our data up to 25 GHz, no good result can be obtained. It should be noted that estimation of  $\varepsilon_\infty$  critically depends on the high-frequency limit of the data. The value of  $\varepsilon_\infty = 4.8$  is best to fit our data up to 25 GHz. Our value of  $\varepsilon_\infty = 4.8$  and Barthel value of  $\Delta\varepsilon_3 + \varepsilon_\infty$ <sup>18,19</sup> are identical.

## C. Methanol–water mixtures

Dielectric relaxation measurements for methanol–water mixtures were carried out at 20, 25, and 30 °C. Data accumulation was thoroughly made. We made efforts to obtain as accurate data as possible at each measured point. Figure 2 shows dielectric relaxation for the methanol–water mixtures at 25 °C at various concentrations. A least-squares best fitting procedure was performed by using various models in Eq. (1). The values of  $\varepsilon_\infty$  for the mixtures were determined approximately according to the following function:

$$\varepsilon_\infty = X_v \cdot \varepsilon_{\infty(w)} + (1 - X_v) \varepsilon_{\infty(MA)}, \quad (3)$$

TABLE I. Summary of the results of the fitting procedure using various models. Dielectric relaxation parameters in Eq. (1) for methanol–water mixtures at various concentrations and temperatures with the normalized variance  $V_{\text{norm}}$  are listed.

Model	$\Delta\varepsilon_1$	$\log \tau_1$	$\log \tau_m$	$\alpha_1$	$\beta_1$	$\Delta\varepsilon_2$	$\log \tau_2$	$\varepsilon_\alpha$	$V_{\text{norm}} \times 10^3$
[1] $X=0.035$ at 25 °C									
(a)CC1	70.44	-11.017	-11.017	1.000	0.994	...	...	5.2	0.0997
(b)HN1	70.44	-11.017	-11.017	1.000	0.994	...	...	5.2	0.0997
(c)D1	70.21	-11.016	-11.016	1.000	1.000	...	...	5.2	0.1117
(d)DC1	70.25	-11.008	-11.010	0.995	1.000	...	...	5.2	0.1428
[2] $X=0.2$ at 20 °C									
(a)CC1	60.09	-10.722	-10.722	1.000	0.961	...	...	5.3	0.0424
(b)HN1	70.00	-10.712	-10.721	0.989	0.964	...	...	5.3	0.0399
(c)DC1	69.67	-10.670	-10.707	0.899	1.000	...	...	5.3	0.1602
[3] $X=0.7$ at 25 °C									
(a)CC2	33.54	-10.389	-10.389	1.000	0.971	2.11	-11.188	4.8	0.0579
(b)DC1	35.48	-10.332	-10.392	0.839	1.000	...	...	4.8	0.1128
(c)HN1	35.62	-10.349	-10.397	0.871	0.984	...	...	4.8	0.0914
(d)CC1	35.85	-10.417	-10.417	1.000	0.939	...	...	4.8	0.2982
[4] $X=0.9$ at 20 °C									
(a)CC2	29.72	-10.258	-10.258	1.000	0.979	1.41	-11.145	4.9	0.0514
(b)DC1	31.06	-10.211	-10.260	0.867	1.000	...	...	4.9	0.0809
(c)HN1	31.06	-10.211	-10.260	0.867	1.000	...	...	4.9	0.0809
(d)CC1	31.39	-10.278	-10.278	1.000	0.948	...	...	4.9	0.2481
[5] $X=1.0$ at 25 °C									
(a)D2	25.45	-10.291	-10.291	1.000	1.000	1.25	-11.140	4.8	0.0633
(b)DC1	27.74	-10.269	-10.298	0.918	1.000	...	...	4.8	0.0634
(c)HN1	27.74	-10.269	-10.298	0.918	1.000	...	...	4.8	0.0634
(d)CC1	27.90	-10.309	-10.309	1.000	0.970	...	...	4.8	0.1195
[6] Ethanol at 25 °C <sup>a</sup>									
(a)D2	19.88	-9.787	-9.787	1.000	1.000	0.86	-11.045	3.7	0.0812
(b)DC1	20.80	-9.744	-9.784	0.891	1.000	...	...	3.7	0.1760
(c)HN1	20.80	-9.744	-9.784	0.891	1.000	...	...	3.7	0.1760
(d)CC1	21.01	-9.797	-9.797	1.000	0.958	...	...	3.7	0.4534

<sup>a</sup>Reference 12.

where  $\varepsilon_{\infty(W)}$  and  $\varepsilon_{\infty(MA)}$  are the high-frequency permittivity limits for pure water and methanol, respectively, and  $X_V$  is the volume fraction of water. The values of  $\varepsilon_{\infty(W)}$  and  $\varepsilon_{\infty(MA)}$  used in this study are 5.2 and 4.8 at 25 °C, respectively. We believe that this assumption is one very good way

to determine the value of  $\varepsilon_{\infty}$  for the mixtures to explain dielectric behavior in the microwave region. A summary of the results of the fitting procedure using various models is listed in Table I in order to provide statistical information for choosing appropriate models.

According to other studies,<sup>13–15</sup> dielectric spectra for various alcohol–water mixtures including methanol–water are asymmetric for the entire concentration range, and well described by the Davidson–Cole model or sometimes the more complicated Havriliak–Negami model. It is found in this study that dielectric spectra of the methanol–water mixtures in the concentrated region of  $X \geq 0.4$  are asymmetric and broader on the high-frequency side, which is consistent

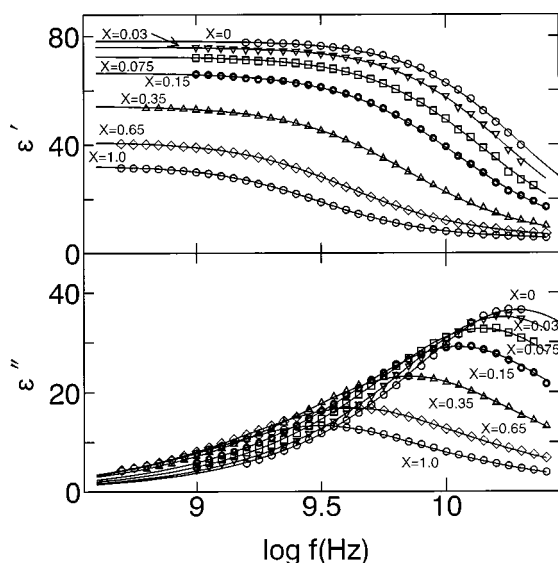


FIG. 2. Frequency dependence of dispersion ( $\varepsilon'$ ) and absorption ( $\varepsilon''$ ) for the methanol–water mixtures at 25 °C expressed in 0.05 steps in  $\log f$  at various concentrations. The solid curves are calculated from Eq. (4).

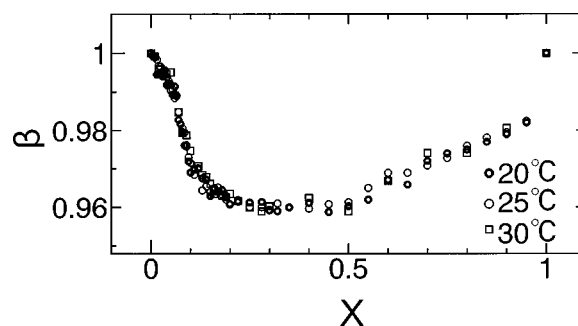


FIG. 3. Plots of the Cole–Cole parameters  $\beta$  in Eq. (4) against molar fraction of methanol  $X$  for the methanol–water mixtures at 20 and 25 °C.

TABLE II. Dielectric relaxation parameters in Eq. (4) for methanol-water mixtures at various concentrations at 20, 25, and 30 °C.

$X$	$\Delta\epsilon_1$	$\log \tau_1$ (exp)	$\log \tau_1$ (calc)	$\beta_1$	$\Delta\epsilon_2$	$\log \tau_2$	$\epsilon_\infty$	$X$	$\Delta\epsilon_1$	$\log \tau_1$ (exp)	$\log \tau_1$ (calc)	$\beta_1$	$\Delta\epsilon_2$	$\log \tau_2$	$\epsilon_\infty$
20 °C															
0.00	75.10	-11.032	-11.032	1.000	...	...	5.3	0.08	67.16	-10.941	-10.941	0.981	...	...	5.2
0.005	74.69	-11.023	-11.023	0.999	...	...	5.3	0.085	66.73	-10.935	-10.934	0.979	...	...	5.2
0.01	74.51	-11.014	-11.014	0.999	...	...	5.3	0.09	66.59	-10.928	-10.928	0.976	...	...	5.2
0.015	73.89	-11.004	-11.005	0.995	...	...	5.3	0.095	66.00	-10.921	-10.921	0.973	...	...	5.2
0.02	73.47	-10.994	-10.995	0.995	...	...	5.3	0.10	65.54	-10.914	-10.914	0.972	...	...	5.2
0.025	73.10	-11.984	-10.984	0.995	...	...	5.3	0.11	65.04	-10.900	-10.899	0.968	...	...	5.2
0.03	72.74	-10.973	-10.974	0.994	...	...	5.3	0.12	64.17	-10.885	-10.885	0.970	...	...	5.2
0.035	72.30	-10.963	-10.963	0.995	...	...	5.3	0.13	63.37	-10.872	-10.872	0.964	...	...	5.2
0.04	72.13	-10.953	-10.952	0.992	...	...	5.3	0.14	62.89	-10.859	-10.859	0.965	...	...	5.2
0.045	71.75	-10.942	-10.942	0.992	...	...	5.3	0.15	61.88	-10.846	-10.846	0.964	...	...	5.2
0.05	71.64	-10.932	-10.932	0.992	...	...	5.3	0.16	61.43	-10.833	-10.833	0.965	...	...	5.2
0.055	71.13	-10.922	-10.922	0.989	...	...	5.3	0.17	60.86	-10.822	-10.821	0.965	...	...	5.2
0.06	70.70	-10.913	-10.913	0.991	...	...	5.3	0.18	60.03	-10.809	-10.809	0.963	...	...	5.2
0.065	70.35	-10.903	-10.904	0.989	...	...	5.3	0.19	59.30	-10.797	-10.798	0.962	...	...	5.1
0.07	70.00	-10.896	-10.896	0.983	...	...	5.3	0.20	58.76	-10.786	-10.786	0.961	...	...	5.1
0.075	69.52	-10.888	-10.889	0.982	...	...	5.3	0.22	57.63	-10.763	-10.763	0.962	...	...	5.1
0.08	69.18	-10.882	-10.882	0.980	...	...	5.3	0.25	55.71	-10.730	-10.730	0.960	...	...	5.1
0.085	68.87	-10.875	-10.875	0.976	...	...	5.3	0.28	54.15	-10.699	-10.699	0.960	...	...	5.1
0.09	68.07	-10.868	-10.868	0.976	...	...	5.2	0.30	52.93	-10.680	-10.681	0.959	...	...	5.0
0.095	67.80	-10.861	-10.861	0.972	...	...	5.2	0.32	51.80	-10.664	-10.664	0.961	...	...	5.0
0.10	67.36	-10.854	-10.853	0.969	...	...	5.2	0.35	49.77	-10.641	-10.641	0.960	...	...	5.0
0.11	66.54	-10.839	-10.838	0.970	...	...	5.2	0.40	46.66	-10.603	-10.603	0.960	1.05	-11.208	4.9
0.12	65.91	-10.823	-10.823	0.970	...	...	5.2	0.45	44.37	-10.565	-10.565	0.961	1.45	-11.205	4.9
0.13	65.32	-10.808	-10.808	0.968	...	...	5.2	0.50	41.85	-10.527	-10.527	0.961	1.68	-11.202	4.9
0.14	64.63	-10.794	-10.794	0.967	...	...	5.2	0.55	39.36	-10.490	-10.490	0.965	1.92	-11.200	4.9
0.15	63.61	-10.780	-10.781	0.963	...	...	5.2	0.60	36.94	-10.453	-10.453	0.969	2.20	-11.196	4.9
0.16	62.83	-10.767	-10.768	0.965	...	...	5.2	0.65	34.85	-10.418	-10.418	0.969	2.13	-11.192	4.8
0.17	62.10	-10.756	-10.756	0.964	...	...	5.2	0.70	33.54	-10.389	-10.389	0.971	2.11	-11.188	4.8
0.18	61.56	-10.744	-10.744	0.965	...	...	5.2	0.75	32.02	-10.366	-10.365	0.973	1.92	-11.181	4.8
0.19	61.04	-10.733	-10.733	0.963	...	...	5.2	0.80	30.35	-10.345	-10.344	0.976	1.88	-11.175	4.8
0.20	60.09	-10.722	-10.722	0.961	...	...	5.2	0.85	29.04	-10.326	-10.327	0.978	1.56	-11.166	4.8
0.22	59.33	-10.701	-10.700	0.962	...	...	5.2	0.90	28.52	-10.312	-10.312	0.979	1.45	-11.160	4.8
0.25	57.51	-10.669	-10.669	0.961	...	...	5.2	0.95	27.15	-10.300	-10.300	0.983	1.38	-11.150	4.8
0.28	55.90	-10.641	-10.640	0.961	...	...	5.2	1.00	26.45	-10.291	-10.291	1.000	1.27	-11.140	4.8
0.30	55.17	-10.623	-10.623	0.959	...	...	5.2	30 °C							
0.32	53.80	-10.607	-10.607	0.959	...	...	5.2	0.00	71.10	-11.135	-11.134	1.000	...	...	5.1
0.35	51.95	-10.583	-10.584	0.960	...	...	5.1	0.01	70.80	-11.118	-11.117	0.999	...	...	5.1
0.40	47.81	-10.545	-10.545	0.961	1.20	-11.195	5.1	0.02	69.99	-11.098	-11.099	0.996	...	...	5.1
0.45	45.50	-10.507	-10.507	0.959	1.48	-11.191	5.1	0.03	69.44	-11.081	-11.080	0.995	...	...	5.1
0.50	43.00	-10.470	-10.470	0.960	1.75	-11.188	5.0	0.04	68.62	-11.061	-11.062	0.995	...	...	5.1
0.55	40.51	-10.433	-10.433	0.962	2.07	-11.185	5.0	0.05	67.83	-11.043	-11.044	0.995	...	...	5.1
0.60	38.19	-10.396	-10.396	0.967	2.24	-11.182	5.0	0.06	66.88	-11.028	-11.028	0.989	...	...	5.1
0.65	36.01	-10.360	-10.361	0.966	2.18	-11.178	4.9	0.07	66.24	-11.014	-11.013	0.986	...	...	5.1
0.70	34.67	-10.333	-10.332	0.972	2.15	-11.173	4.9	0.08	65.52	-11.001	-11.000	0.980	...	...	5.1
0.75	33.00	-10.310	-10.309	0.974	1.91	-11.169	4.9	0.09	64.83	-10.988	-10.988	0.979	...	...	5.1
0.80	31.82	-10.289	-10.290	0.975	1.89	-11.163	4.9	0.10	63.80	-10.974	-10.974	0.975	...	...	5.1
0.85	30.42	-10.272	-10.272	0.977	1.66	-11.157	4.9	0.11	63.23	-10.960	-10.961	0.970	...	...	5.1
0.90	29.72	-10.258	-10.258	0.979	1.41	-11.145	4.9	0.12	61.84	-10.947	-10.948	0.971	...	...	5.1
0.95	28.29	-10.248	-10.247	0.982	1.35	-11.135	4.9	0.13	61.50	-10.935	-10.935	0.968	...	...	5.0
1.00	27.10	-10.239	-10.239	1.000	1.28	-11.125	4.9	0.14	61.18	-10.921	-10.922	0.968	...	...	5.0
25 °C															
0.00	73.10	-11.083	-11.083	1.000	...	...	5.2	0.15	60.60	-10.910	-10.910	0.966	...	...	5.0
0.005	72.75	-11.075	-11.074	0.999	...	...	5.2	0.16	60.09	-10.898	-10.898	0.963	...	...	5.0
0.01	72.45	-11.066	-11.066	0.999	...	...	5.2	0.17	59.56	-10.886	-10.886	0.964	...	...	5.0
0.015	72.01	-11.056	-11.056	0.998	...	...	5.2	0.18	58.83	-10.874	-10.874	...	...	5.0	
0.02	71.71	-11.046	-11.047	0.997	...	...	5.2	0.19	58.09	-10.862	-10.862	0.961	...	...	5.0
0.025	71.19	-11.037	-11.037	0.997	...	...	5.2	0.20	56.86	-10.849	-10.850	0.964	...	...	5.0
0.03	70.93	-11.026	-11.027	0.995	...	...	5.2	0.22	55.82	-10.825	-10.826	0.962	...	...	5.0
0.035	70.44	-11.017	-11.017	0.994	...	...	5.2	0.25	54.15	-10.789	-10.790	0.960	...	...	5.0
0.04	70.18	-11.008	-11.007	0.994	...	...	5.2	0.28	52.90	-10.757	-10.757	0.959	...	...	5.0
0.045	69.84	-10.997	-10.997	0.993	...	...	5.2	0.30	51.95	-10.738	-10.737	0.960	...	...	5.0
0.05	69.58	-10.987	-10.988	0.991	...	...	5.2	0.40	46.46	-10.660	-10.660	0.962	1.21	-11.220	4.9
0.055	69.10	-10.980	-10.979	0.991	...	...	5.2	0.50	40.65	-10.584	-10.585	0.959	1.70	-11.210	4.9
0.06	68.79	-10.970	-10.970	0.998	...	...	5.2	0.60	35.91	-10.510	-10.510	0.967	2.23	-11.202	4.8
0.065	68.57	-10.962	-10.962	0.989	...	...	5.2	0.70	32.30	-10.445	-10.445	0.974	1.95	-11.200	4.7
0.07	68.04	-10.954	-10.955	0.985	...	...	5.2	0.80	29.70	-10.399	-10.399	0.974	1.70	-11.190	4.7
0.075	67.44	-10.947	-10.948	0.982	...	...	5.2	0.90	28.02	-10.364	-10.364	0.981	1.31	-11.165	4.7
								1.00	25.79	-10.343	-10.343	1.000	1.10	-11.160	4.7

with the results of other studies,<sup>13–15</sup> but in the region of  $0 \leq X < 0.4$ , the spectra are nearly symmetric in the measured frequency range.

### 1. Concentrated region of $X \geq 0.4$

In the region of  $X \geq 0.4$ , among the one-process models, the Davidson–Cole (DC1) model is suitable for representation of the data, giving small variance. Considering the fact that superposition of the two Debye processes ( $\alpha_j = \beta_j = 1$ ,  $n = 2$ ) gives the best description of the dielectric behavior of pure methanol up to 25 GHz and this model has well assigned physical background, the high-frequency process ( $j = 2$ ) characterized by  $\tau_2$ , which is attributed to reorientation of methanol monomer at the ends of the chainlike structures, is also expected to exist for the mixtures in the concentrated region.

As with the results of the fitting procedure using various two-process models, dielectric relaxation for the mixtures in the region of  $0.4 \leq X \leq 1.0$  can be well described by the two-process model represented by the following function:

$$\varepsilon^*(\omega) = \varepsilon_\infty + \frac{\Delta\varepsilon_1}{1 + (j\omega\tau_1)^\beta} + \frac{\Delta\varepsilon_2}{1 + j\omega\tau_2}. \quad (4)$$

Examples [3] and [4] in Table I clearly show that the model represented by Eq. (4) gives the best description of the data. The value of  $\beta$  decreases from unity for pure methanol (at  $X = 1$ ) with increasing water content. Adding water to methanol brings about distribution of the relaxation time. The relaxation strength for the higher frequency process,  $\Delta\varepsilon_2$ , gradually increases with decreasing  $X$ , and reaches a maximum at  $X \sim 0.65$ . After that,  $\Delta\varepsilon_2$  decreases with decreasing  $X$ .

### 2. Water-rich region of $0 \leq X < 0.4$

In the region of  $X < 0.4$ ,  $\Delta\varepsilon_2$  in Eq. (4) converges to zero as the results of the fitting procedure. The higher frequency process can not be separated, though it may also exist. The single Cole–Cole ( $\alpha_j = 1$ ,  $0 < \beta_j \leq 1$ ,  $n = 1$ ) model provides very good fit in this region. Plots of the Cole–Cole parameter  $\beta$  are shown in Fig. 3. In the dilute region of  $0 \leq X \leq 0.07$ , the spectra of the mixtures are nearly the Debye type. The value of  $\beta$  decreases from unity for pure water (at  $X = 0$ ) with increasing methanol concentration  $X$ , and reaches minimum at  $X \sim 0.4$ , being almost constant in the region of  $0.3 \leq X \leq 0.5$ . If the Havriliak–Negami model including two shape parameters  $\alpha$  and  $\beta$  is used with the values of  $\varepsilon_\infty$  determined by Eq. (3) in the region of  $0 \leq X < 0.4$ , the asymmetric parameter  $\alpha$  converges to unity. If  $\varepsilon_\infty$  is treated as a random parameter, the value of  $\alpha$  is not reliable as a measure of asymmetrical shape of the spectra because  $\varepsilon_\infty$  and  $\alpha$  strongly correlate with each other.<sup>12</sup> The truth is that, as proved by the fact that the Cole–Cole model using the value of  $\varepsilon_\infty$  determined according to Eq. (3) gives very good fit, the spectra in the region of  $0 \leq X < 0.4$  in the measured frequency range are nearly symmetric.

Dielectric parameters in Eq. (4) at various concentrations and temperatures are listed in Table II. Plots of the logarithm of the relaxation time for the main process,  $\log \tau_1$ , against  $X$  are shown in Fig. 4. Figure 4(b) is an enlarged view in the

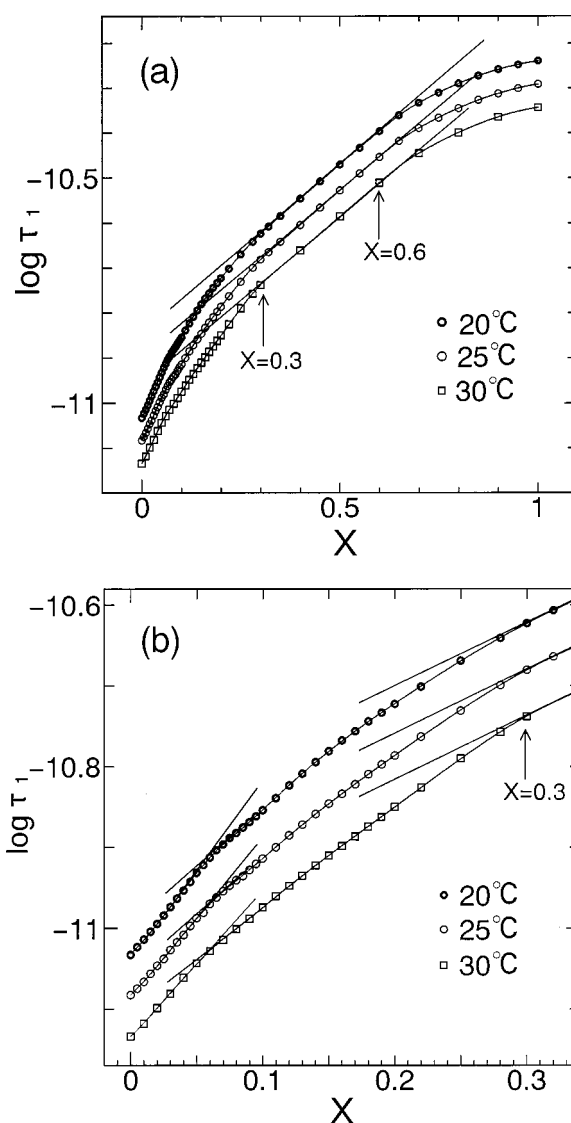


FIG. 4. Plots of  $\log \tau_1$  against molar fraction of methanol  $X$  for the methanol–water mixtures at 20 and 25 °C. Figure 4(b) is an enlarged view in the dilute region.

dilute region. Figure 4(a) shows that there exist two regions in  $\log \tau_1$  bound at  $X \sim 0.3$ . The boundary shifts toward the higher concentration side than that for the ethanol–water system,  $X \sim 0.18$ .<sup>12</sup> In the region of  $0.3 \leq X \leq 0.6$ ,  $\log \tau_1(X)$  is an almost completely linear function of  $X$  at various temperatures, and exhibits a clear change at  $X \sim 0.6$ . As Fig. 4(b) shows, plots of  $\log \tau_1$  in a water-rich region exhibit complicated behavior. In the region of  $0.05 \leq X \leq 0.08$ ,  $\partial(\log \tau_1)/\partial X$  gets rapidly smaller with increasing  $X$ . In the region of  $0 \leq X \leq 0.16$ ,  $\partial(\log \tau_1)/\partial X$  becomes larger at lower temperature, but in the region of  $0.16 \leq X \leq 0.3$ , it becomes smaller at lower temperature. The phenomena observed are essentially important and directly correspond to the characteristic behaviors of the activation enthalpy  $\Delta H$  of the mixtures in the region below  $X \sim 0.3$ , which will be explained in detail in the next section.

## IV. DISCUSSION

According to the Eyring formula,<sup>23</sup> the relaxation time  $\tau$  is given by

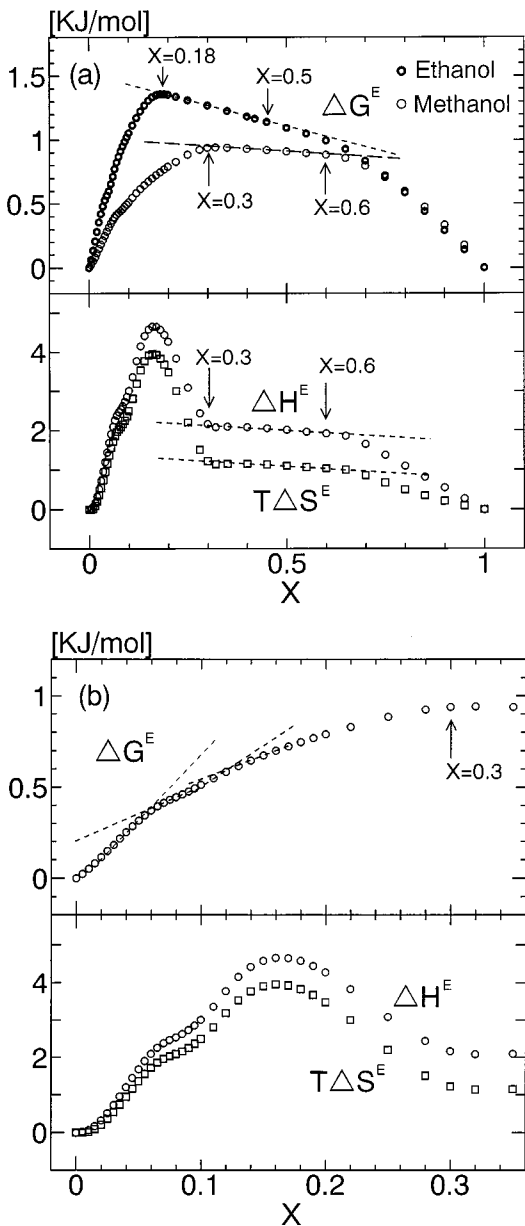


FIG. 5. Concentration dependence of the excess (integral) activation free energy  $\Delta G^E$ , enthalpy  $\Delta H^E$ , and entropy  $\Delta S^E$  for the methanol–water mixtures at 25 °C plotted against the molar fraction of ethanol  $X$ . Figure 5(b) is an enlarged view in the dilute region.

$$\tau = \frac{h}{kT} \exp\left(\frac{\Delta G}{RT}\right) = \frac{h}{kT} \exp\left(\frac{\Delta H}{RT}\right) \exp\left(\frac{-\Delta S}{R}\right), \quad (5)$$

where  $h$  is the Planck constant,  $k$  is the Boltzmann constant,  $R$  is the gas constant,  $T$  is the absolute temperature,  $\Delta G$  is the activation free energy,  $\Delta H$  is the activation enthalpy, and  $\Delta S$  is the activation entropy. There is a relation  $\Delta G = \Delta H - T\Delta S$ . These quantities at the concentration  $X$  are experimentally obtained from the concentration and temperature dependences of the relaxation time for the main process  $\tau_1$  using the following equations:

$$\Delta G(X) = RT[\ln \tau_1(X) - \ln(h/kT)], \quad (6)$$

$$\Delta H(X) = \frac{\partial(\Delta G(X)/T)}{\partial(1/T)} = R \left[ \frac{\partial \ln \tau_1(X)}{\partial(1/T)} \right] - RT, \quad (7)$$

$$T\Delta S(X) = \Delta H(X) - \Delta G(X). \quad (8)$$

$\Delta G(X)$ ,  $\Delta H(X)$ , and  $\Delta S(X)$  for the main process ( $j=1$ ) were calculated by graphically differentiating the smooth curves shown in Fig. 4 obtained by the  $B$ -spline fitting procedure.

If the mixture is an ideal system,  $\Delta G$ ,  $\Delta H$ , and  $\Delta S$  will be given by

$$\Delta F(X) = X\Delta F_{MA0} + (1-X)\Delta F_{W0} \quad \text{for } \Delta F = \Delta G, \Delta H, \text{ and } \Delta S, \quad (9)$$

where  $X$  is the molar fraction of methanol, and  $\Delta F_{MA0}$  and  $\Delta F_{W0}$  denote the activation free energy, enthalpy, or entropy for pure methanol and water for the main process ( $j=1$ ), respectively. In the case of the actual mixtures, large excess contributions were observed. The excess activation free energy  $\Delta G^E$ , enthalpy  $\Delta H^E$ , and entropy  $\Delta S^E$  are given by

$$\Delta F^E(X) = \Delta F(X) - [X\Delta F_{MA0} + (1-X)\Delta F_{W0}] \quad \text{for } \Delta F^E = \Delta G^E, \Delta H^E, \text{ and } \Delta S^E. \quad (10)$$

There is a relation,  $\Delta G^E = \Delta H^E - T\Delta S^E$ . The large excess contributions are considered to be the results of multiple interactions between methanol and water. Figures 5(a) and 5(b) show plots of the excess quantities,  $\Delta G^E$ ,  $\Delta H^E$ , and  $T\Delta S^E$  against  $X$  calculated from the data of the relaxation times at 20 and 25 °C. Figure 5(b) is an enlarged view in dilute region. All the excess quantities take positive values for the entire concentration range. It was confirmed that the values of  $\Delta H^E$  and  $\Delta S^E$  calculated from the various combinations of the data at 20 and 25 °C, at 25 and 30 °C, and at 20 and 30 °C, agree well with each other, while the values of  $\Delta H^E$  and  $\Delta S^E$  become slightly larger at lower temperature. Figure 5(a) shows that there exist two regions separated by the boundary of  $X \sim 0.3$  in which behaviors of the excess molar quantities are quite different from each other. In the region of  $0 \leq X \leq 0.3$ ,  $\Delta H^E$  and  $\Delta S^E$  sharply depend on  $X$ , and exhibit maxima at  $X \sim 0.16$ . The large excess contributions in the water-rich region must be structural in origin. The maxima in  $\Delta H^E$  and  $\Delta S^E$  at  $X \sim 0.16$  indicate that total intermolecular interactions including water–methanol, water–water, and methanol–methanol become largest at  $X \sim 0.16$  in terms of the activation enthalpy and entropy. However,  $\Delta G^E$  does not attain its maximum at  $X \sim 0.16$  due to an alternative compensation between  $\Delta H^E$  and  $\Delta S^E$ . In the region of  $0 \leq X \leq 0.3$ ,  $\Delta G^E$  increases with increasing  $X$ , and reaches a maximum at  $X \sim 0.3$ . In other words,  $\Delta H^E$  against  $\Delta S^E$  reaches a maximum. Methanol and water molecules form the most stable clusters at the point. In the region of  $X \geq 0.3$ ,  $\Delta G^E$  decreases with increasing  $X$ .

In the case of the ethanol–water system,<sup>12</sup>  $\Delta G^E$  reaches a maximum at  $X \sim 0.18$ , and  $\Delta H^E$  and  $\Delta S^E$  at  $X \sim 0.11$ . The concentrations at which the excess molar quantities exhibit maxima shift higher values of  $X$  in the case of the methanol–water system. The maximum values of  $\Delta G^E$  for the methanol–water system are smaller, about 70% of that for the ethanol–water system, but, in the region of  $X \geq 0.7$ ,  $\Delta G^E$  for the two systems take almost the same values.

As shown in Fig. 5(b), in the water-rich region, two modes of increase in  $\Delta H^E$  and  $\Delta S^E$  appear, indicating the existence of two types of contributions of methanol to  $\Delta H^E$  and  $\Delta S^E$ . The changeover from one mixing scheme of water and methanol to the other seems to occur in this region. Here, we introduce the evaluation of the excess partial molar quantities, which correspond to the substantial contribution of each component to the excess integral quantities,  $\Delta G^E$ ,  $\Delta H^E$ , and  $\Delta S^E$ .

The excess partial molar activation energy, enthalpy, and entropy for methanol,  $\Delta G_{MA}^E$ ,  $\Delta H_{MA}^E$ , and  $\Delta S_{MA}^E$ , are given by

$$\begin{aligned}\Delta F_{MA}^E &= \left( \frac{\partial \{ (n_{MA} + n_W) \Delta F^E \}}{\partial n_{MA}} \right) \\ &= \Delta F^E + (1-X) \left( \frac{\partial \Delta F^E}{\partial X} \right), \\ \text{for } \Delta F_{MA}^E &= \Delta G_{MA}^E, \Delta H_{MA}^E, \text{ and } \Delta S_{MA}^E,\end{aligned}\quad (11)$$

where  $n_{MA}$  and  $n_W$  are molar number of ethanol and water.

The excess partial molar activation energy, enthalpy, and entropy for water,  $\Delta G_W^E$ ,  $\Delta H_W^E$ , and  $\Delta S_W^E$ , are given by

$$\begin{aligned}\Delta F_W^E &= \left( \frac{\partial \{ (n_{MA} + n_W) \Delta F^E \}}{\partial n_W} \right) \\ &= \Delta F^E - X \left( \frac{\partial \Delta F^E}{\partial X} \right), \\ \text{for } \Delta F_W^E &= \Delta G_W^E, \Delta H_W^E, \text{ and } \Delta S_W^E.\end{aligned}\quad (12)$$

The excess partial molar quantities for methanol,  $\Delta G_{MA}^E$ ,  $\Delta H_{MA}^E$ , and  $\Delta S_{MA}^E$ , and those for water  $\Delta G_W^E$ ,  $\Delta H_W^E$ , and  $\Delta S_W^E$  plotted against  $X$  are shown in Figs. 6(a) and 6(b). Figure 6(b) is an enlarged view in the dilute region.

### A. Water-rich region of $0 \leq X \leq 0.3$

In the region of  $0 \leq X \leq 0.16$ ,  $\Delta H_{MA}^E$  and  $\Delta S_{MA}^E$  take large positive values. This means that methanol molecules play a role of drastically enlarging the activation enthalpy  $\Delta H$  and entropy  $\Delta S$  of the system. This is clearly attributed to the structural enhancement of the hydrogen bond network of water, the so-called hydrophobic hydration. The linear relation between  $\Delta H_{MA}^E$  and  $\Delta S_{MA}^E$  is consistent with the idea of enthalpy–entropy compensation.<sup>24</sup>  $\Delta H_{MA}^E$  and  $\Delta S_{MA}^E$  show sharp maxima at  $X=0.045$  and  $X=0.12$ , as shown in Fig. 6(b), which is associated with the two modes of increase in the excess integral quantities,  $\Delta H^E$  and  $\Delta S^E$ . The behaviors of the partial molar quantities for the methanol–water system and those for the ethanol–water system<sup>12</sup> are in part quite similar to each other. In the case of the ethanol–water system, the maxima in the excess partial molar quantities for ethanol,  $\Delta H_{EA}^E$  and  $\Delta S_{EA}^E$ , appear at  $X=0.04$  and  $X=0.08$ ,<sup>12</sup> which shift toward lower values of  $X$  than those for methanol,  $\Delta H_{MA}^E$  and  $\Delta S_{MA}^E$ . Judging from the fact that the two maxima in  $\Delta H_{MA}^E$  and  $\Delta S_{MA}^E$  appear, it is not doubted that mixing schemes of methanol and water around the two points  $X=0.045$  and  $X=0.12$  are qualitatively different from

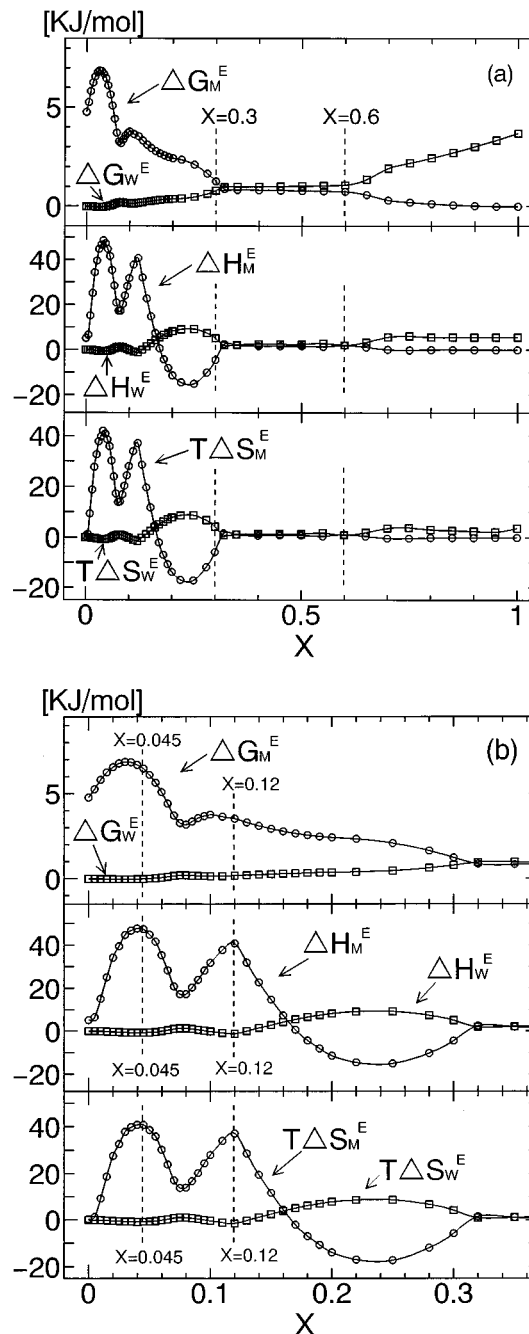


FIG. 6. Concentration dependence of the excess partial molar activation free energy, enthalpy, and entropy for methanol,  $\Delta G_{MA}^E$ ,  $\Delta H_{MA}^E$ , and  $\Delta S_{MA}^E$ , and those for water,  $\Delta G_W^E$ ,  $\Delta H_W^E$ , and  $\Delta S_W^E$  at 25 °C plotted against the molar fraction of methanol  $X$ . (b) is an enlarged view in the dilute region.

each other. The two singular concentrations  $X=0.045$  and  $X=0.12$  can be explained as saturation points of structure formation.

In the region of  $0 \leq X \leq 0.045$ , the derivatives of  $\Delta H_{MA}^E$  and  $\Delta S_{MA}^E$ ,  $\partial \Delta H_{MA}^E / \partial X$  and  $\partial \Delta S_{MA}^E / \partial X$ , take positive, which supports the following two views: (1) The hydrogen bond network of water is more enhanced, as an average distance between methanol molecules becomes shorter when more than 21 water molecules per 1 methanol molecule exist in the mixtures. (2) The hydration shells become more rigid around methanol molecules when close location of two or

more methanol molecules occurs via the water network or by occupying one large cavity of the three-dimensional water network than those are when methanol molecules are independently surrounded by water molecules.

It was reported that 20 water molecules are needed to form three-dimensional spherical water cages.<sup>25-27</sup> The ratio of 1 methanol and 20 water corresponds to  $X \sim 0.048$ . The concentration at which the first maximum in  $\Delta H_{MA}^E$  and  $\Delta S_{MA}^E$  appear,  $X = 0.045$ , being a bit higher than but very close to that in  $\Delta H_{EA}^E$  and  $\Delta S_{EA}^E$ ,  $X = 0.04$ ,<sup>12</sup> is very close to  $X \sim 0.048$ . It is therefore suggested that steep increases of  $\Delta H_{MA}^E$  and  $\Delta S_{MA}^E$  in the region of  $0 \leq X \leq 0.045$  are attributed to the clathrate hydration shell formation around methanol molecules, and the structural enhancement in this scheme becomes saturated at  $X = 0.045$ . The maximum values in  $\Delta H_{MA}^E$  and  $\Delta S_{MA}^E$  are about 50% of those in  $\Delta H_{EA}^E$  and  $\Delta S_{EA}^E$ .<sup>12</sup> This finding clearly indicates that the size of hydrophobic group largely determines an ability of alcohol in the structural enhancement of the hydrogen bond networks of water. The ethanol molecule has more than two times larger an effect on the hydrophobic hydration than methanol molecule.

Methanol addition to the mixture with  $X = 0.045$  makes the derivatives  $\partial \Delta H_{MA}^E / \partial X$  and  $\partial \Delta S_{MA}^E / \partial X$  turn negative. At  $X = 0.045$ , breakage of the clathrate hydration shell seems to begin to take place due to lack of water molecules to form the clathrate cages for all the methanol molecules. At  $X = 0.08$ ,  $\Delta H_{MA}^E$  and  $\Delta S_{MA}^E$  begin to increase again, and reach maxima at  $X = 0.12$  as shown in Fig. 6(b). The changeover from one mixing scheme to the other occurs around  $X \sim 0.08$ . This finding strongly suggests that, in the region of  $0.08 \leq X \leq 0.12$ , structural enhancement in the new scheme goes on, and  $X = 0.12$  is the saturation point of the enhancement in this scheme. It should be noted that  $X = 0.12$  is very close to the concentration at which partial molar volume of methanol in the mixtures shows a minimum,<sup>2</sup> indicating that methanol molecules are already associated and most be closely located to each other at  $X \sim 0.12$ . It is thus suggested that a steep increase of  $\Delta H_{MA}^E$  and  $\Delta S_{MA}^E$  in the region of  $0.08 \leq X \leq 0.12$  is attributed to reformation of hydration water shells accompanied by molecular association of methanol. The shape and size of the hydration shells will be quite different from the clathrate shells existing in the region of  $0 < X \leq 0.045$ .

In the region of  $X > 0.12$ ,  $\Delta H_{MA}^E$  and  $\Delta S_{MA}^E$  steeply decrease, and turn negative at  $X \sim 0.17$ . In the region of  $0.17 < X < 0.3$ ,  $\Delta H_{MA}^E$  and  $\Delta S_{MA}^E$  take negative values, while the excess integral quantities,  $\Delta H^E$  and  $\Delta S^E$ , still remain large and positive. The negative values of  $\Delta H_{MA}^E$  and  $\Delta S_{MA}^E$  mean that methanol molecules play a role of largely decreasing the activation enthalpy  $\Delta H$  and entropy  $\Delta S$  of the systems in this region. This suggests that methanol addition to the mixture with  $X \sim 0.12$  leads to abrupt breakage of the saturated hydration structures. A probable explanation is that the hydrogen bond network of water is disrupted by adding methanol. Steric effects of methanol chainlike structures will make it difficult for an insufficient number of water molecules to form three-dimensional networks, and the percolation nature of water will be no longer present in the region of  $X$

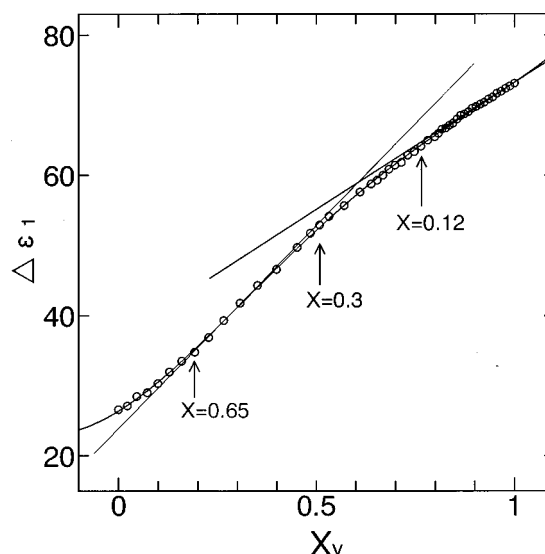


FIG. 7. Plots of the relaxation strength of the main process  $\Delta \epsilon_1$  against the volume fraction of water  $X_v$  for the methanol-water mixtures at 25 °C.

$\geq 0.17$ . Water molecules are orientationally ordered around methanol structures, but do not form rigid cages.  $\Delta H_W^E$  and  $\Delta S_W^E$ , which take nearly zero in the region of  $X \leq 0.12$ , begin to increase at  $X \sim 0.12$ . Water molecules highly stabilize methanol chainlike structures in this region.

Figure 7 shows the relaxation strength for the main process  $\Delta \epsilon_1$  at 25 °C plotted against volume fraction of water  $X_v$ .  $\Delta \epsilon_1$  is a linear function of  $X_v$  in the region of  $1.0 \geq X_v \geq 0.765$ , corresponding to the region of  $0 \leq X \leq 0.12$ , and begins to deviate from the straight line at  $X_v \sim 0.765$  ( $X \sim 0.12$ ). In that no change appears at  $X \sim 0.045$ , the relaxation strength is a weaker indicator of structural changes than the relaxation time, but the linearlike behavior in  $\Delta \epsilon_1(X_v)$  suggests that the water structures which cause the strength of pure water to be such a large value of 73.1 (at 25 °C) still remain in the region of  $X \leq 0.12$ .  $\Delta \epsilon_1(X_v)$  exhibits another straight line in the region of  $0.508 \geq X_v \geq 0.193$ , corresponding to the region of  $0.3 \leq X \leq 0.65$ . The intermediate region of  $0.765 \geq X_v \geq 0.508$  ( $0.12 \leq X \leq 0.3$ ), corresponding to the region in which  $\Delta H_{MA}^E$  and  $\Delta S_{MA}^E$  take negative values, is the crossover of the two straight lines in  $\Delta \epsilon_1(X_v)$ , as indicated by Fig. 7.

## B. Concentrated region of $X \geq 0.3$

As shown in Fig. 6(a), the behavior of the excess partial molar quantities in the concentrated region of  $0.3 \leq X \leq 1.0$  is remarkably different from that in the region of  $0 \leq X \leq 0.3$ .  $\Delta H_{MA}^E$  and  $\Delta S_{MA}^E$  take nearly zero in the region of  $0.3 \leq X \leq 1.0$ . This means that, in terms of the activation enthalpy and entropy, methanol molecules in the mixtures are in almost the same environment as they are in pure methanol, associated and forming chainlike clusters.  $\Delta H_W^E$  and  $\Delta S_W^E$  take small but positive values in this region, which means that water molecules stabilize the methanol clusters by surrounding or exothermically attaching to them.

In more detail, all the excess partial molar quantities,  $\Delta G_{MA}^E$ ,  $\Delta H_{MA}^E$ ,  $\Delta S_{MA}^E$ ,  $\Delta G_W^E$ ,  $\Delta H_W^E$ , and  $\Delta S_W^E$ , showing

almost no change in the region of  $0.3 \leq X \leq 0.6$ , exhibit clear changes at  $X \sim 0.6$ . As shown in Fig. 7, the relaxation strength  $\Delta \varepsilon_1$  plotted against volume fraction of water  $X_v$  is a linear function of  $X_v$  in the region of  $0.508 \geq X_v \geq 0.193$  ( $0.3 \leq X \leq 0.65$ ). Both the relaxation time and the strength of the mixtures are determined only by the mixing ratio in this region. This means that states of both methanol and water molecules do not change despite the large variation of methanol to water ratio. The changes in all the excess partial molar quantities at  $X \sim 0.6$  directly correspond to changes in slopes of the excess molar integral quantities,  $\Delta G^E$ ,  $\Delta H^E$ , and  $\Delta S^E$ , as shown in Fig. 5(a). At  $X \sim 0.6$ ,  $\Delta G_{MA}^E$ ,  $\Delta H_{MA}^E$ ,  $\Delta S_{MA}^E$  begin to decrease and reach zero at  $X=1.0$ .  $\Delta G_W^E$ ,  $\Delta H_W^E$ , and  $\Delta S_W^E$  begin to increase at  $X \sim 0.6$ .  $\Delta \varepsilon_1$  plotted against  $X_v$  also shows a change at  $X \sim 0.65$  ( $X_v \sim 0.193$ ) as shown in Fig. 7.  $\Delta \varepsilon_1(X_v)$  exhibits a curved line in the concentrated region of  $0.193 \geq X_v \geq 0$  ( $0.65 \leq X \leq 1.0$ ). Judging from these facts, structures of methanol cluster in the region below and above  $X \sim 0.6$  are somewhat different, due to lack of water molecules to stabilize methanol chainlike clusters.

The higher frequency process ( $j=2$ ) for pure methanol is attributed to reorientation of the monomer situated at the end of the chain.<sup>18,19</sup> As methanol molecules in the mixture form mostly the same chainlike clusters as those in pure methanol in the region of  $0.3 \leq X \leq 1.0$ , as indicated by the fact that  $\Delta H_{MA}^E$  and  $\Delta S_{MA}^E$  take nearly zero, it is reasonable to think that the higher frequency process of the mixtures reflects the similar relaxation mechanism. In the region of  $X \geq 0.6$ , the strength  $\Delta \varepsilon_2$  increases with decreasing  $X$  from  $X=1.0$ , which indicates that water molecules contribute to the higher frequency process. The water molecule will be attached to the hydrophilic site of the methanol molecule at the end of the chain. In the region of  $0.4 \leq X \leq 0.6$ ,  $\Delta \varepsilon_2$  decreases with decreasing  $X$ . This is probably due to the decrease of methanol content.

- <sup>1</sup>F. Franks and H. H. Johnson, *Trans. Faraday Soc.* **58**, 656 (1962).
- <sup>2</sup>K. Nakanishi, *Bull. Chem. Soc. Jpn.* **33**, 793 (1960).
- <sup>3</sup>A. Ben-Naim, *J. Chem. Phys.* **67**, 4884 (1977).
- <sup>4</sup>N. Nishi, K. Koga, C. Ohshima, K. Yamamoto, U. Nagashima, and K. Nagami, *J. Am. Chem. Soc.* **110**, 5246 (1988).
- <sup>5</sup>N. Nishi, S. Takahashi, M. Matsumoto, A. Tanaka, K. Muraya, T. Takamuku, and T. Yamaguchi, *J. Phys. Chem.* **99**, 462 (1995).
- <sup>6</sup>Y. Koga, T. Y. H. Wong, and W. W. Y. Siu, *Thermochim. Acta* **169**, 27 (1990).
- <sup>7</sup>Y. Koga, W. W. Y. Siu, and T. Y. H. Wong, *J. Phys. Chem.* **94**, 7700 (1990).
- <sup>8</sup>Y. Koga, *Solid State Phys. (Tokyo)* **37**, 172 (1995).
- <sup>9</sup>M. S. Skaf and B. M. Ladanyi, *J. Chem. Phys.* **102**, 6542 (1995).
- <sup>10</sup>M. S. Skaf and B. M. Ladanyi, *J. Phys. Chem.* **100**, 18258 (1996).
- <sup>11</sup>M. S. A. Laaksonen, P. G. Kusalik, and I. M. Svishchev, *J. Phys. Chem. A* **101**, 5910 (1997).
- <sup>12</sup>T. Sato, A. Chiba, and R. Nozaki, *J. Chem. Phys.* **110**, 2508 (1999).
- <sup>13</sup>S. Mashimo, T. Umehara, and H. Redlin, *J. Chem. Phys.* **95**, 6257 (1991).
- <sup>14</sup>S. Mashimo and N. Miura, *J. Chem. Phys.* **99**, 9874 (1993).
- <sup>15</sup>J.-Z. Bao, M. L. Swicord, and C. C. Davis, *J. Chem. Phys.* **104**, 4441 (1996).
- <sup>16</sup>T. Sato, H. Niwa, A. Chiba, and R. Nozaki, *J. Chem. Phys.* **108**, 4138 (1998).
- <sup>17</sup>U. Kaatze, *J. Chem. Eng. Data* **34**, 371 (1989).
- <sup>18</sup>J. Barthel, K. Bachhuber, R. Buchner, and H. Hetzenauer, *Chem. Phys. Lett.* **165**, 369 (1990).
- <sup>19</sup>J. Barthel and R. Buchner, *Pure Appl. Chem.* **63**, 1473 (1991).
- <sup>20</sup>R. Nozaki and T. K. Bose, *IEEE Trans. Instrum. Meas.* **39**, 945 (1990).
- <sup>21</sup>W. J. Ellison, K. Lamkaouchi, and J.-M. Moreau, *J. Mol. Liq.* **68**, 171 (1996).
- <sup>22</sup>R. D. Bazman, E. F. Casassa, and R. L. Kay, *J. Mol. Liq.* **73,74**, 397 (1997).
- <sup>23</sup>N. E. Hill, W. E. Vaughan, A. H. Price, and M. Davies, *Dielectric Properties and Molecular Behavior* (Reinhold, London, 1969), pp. 69–71.
- <sup>24</sup>R. Lamry and D. S. Rajender, *Biopolymers* **9**, 1125 (1976).
- <sup>25</sup>J. L. Kassner and D. E. Hagen, *J. Chem. Phys.* **64**, 1860 (1976).
- <sup>26</sup>H. Shinohara, U. Nagashima, H. Tanaka, and N. Nishi, *J. Chem. Phys.* **83**, 4183 (1985).
- <sup>27</sup>U. Nagashima, H. Shinohara, N. Nishi, and H. Tanaka, *J. Chem. Phys.* **84**, 209 (1986).